Available online at www.sciencedirect.com
SCIENCE DIRECT®

Journal of the European Ceramic Society 23 (2003) 1183–1191
www.elsevier.com/locate/jeurceramsoc

Effect of the addition of β-Si_3N_4 nuclei on the thermal conductivity of β-Si_3N_4 ceramics

H. Yokota*, M. Ibukiyama

Research Center, Denki Kagaku Kogyo K.K, 3-5-1 Asahi-cho, Machida-city, 194-8560 Tokyo, Japan

Received 16 November 2001; received in revised form 22 July 2002; accepted 7 August 2002

Abstract

Various microstructures of β-Si_3N_4 were fabricated, with or without the addition of β-Si_3N_4 seed particles to high-purity β-Si_3N_4 powder, using Yb_2O_3 and ZrO_2 as sintering additives, by gas-pressure sintering at 1950 °C for 16 h. The thermal conductivity of the specimen without seeds was 140 $W\cdot(m\cdot K)^{-1}$, and the specimen exhibited a bimodal microstructure with abnormally grown grains. The thermal conductivity of the specimen with 24 vol.% seed addition was 143 $W\cdot(m\cdot K)^{-1}$, and this specimen had the bimodal microstructure with finer grain size than that without the seeded material, but maintained the same amount of large grains ($\geqslant 2$ μm in diameter) as in the specimen without the seeds. This finding indicates that the thermal conductivity of β-Si_3N_4 is controlled by the amount of reprecipitated large grains, rather than by the grain size of the β-Si_3N_4.

Keywords: Grain growth; Grain size; Sintering; Si_3N_4; Thermal conductivity

1. Introduction

Many efforts have been directed toward improving the mechanical properties of sintered Si_3N_4. Tough ceramics have been prepared by developing bimodal microstructures, which have abnormal grain growth in tine and uniform matrix grains. Increased fracture toughness is attributed to crack deflection and crack bridging by the abnormally grown grains.[1–4]

On the other hand, a significant increase in the thermal conductivity of sintered β-Si_3N_4 has been achieved recently by using high-purity raw powders with effective sintering additives.[5–9] The key technology for obtaining high thermal conductivity is to promote grain growth and to align the large β-Si_3N_4 grains at the moment. Either abnormal grain growth or controlled nucleation is required to obtain elongated grains of β-Si_3N_4.[10–16] However, fabrication of these materials requires hot-pressing or hot-isostatic-pressing, an expensive and inefficient method for producing complex components. Larger grains are developed from β-Si_3N_4 particles existing in the raw powder,[17] which makes the morphology and distribution of the grain growth difficult to control. Although Hirao et al.[6] reported that development of texture by adding rodlike β-Si_3N_4 seeds to β-Si_3N_4 ceramics leads to enhanced thermal conductivity, up to 120 $W\cdot(m\cdot K)^{-1}$, along the direction of orientation, such seed preparation might be costly; in addition, a sintered material with anisotropic thermal conductivity is limited in practical use.

Watari et al.[18] reported that the thermal conductivity of β-Si_3N_4 ceramics at room temperature is controlled by the internal defect structure of the grains. Therefore, further improving the purity of the raw powders and developing better processing, to suppress defect formation, would result in increased thermal conductivity for β-Si_3N_4 ceramics and lead to an understanding of the mechanism for high thermal conductivity in β-Si_3N_4 ceramics.

Very recently, Kitayama et al.[19] concluded that mere grain growth couldn't improve thermal conductivity by a prediction model. because of the unique faceting nature of sintered Si_3N_4. Kitayama et al.[20] also concluded that the lattice oxygen content controls the thermal conductivity of β-Si_3N_4 ceramics, just as in AlN ceramics. Purification of lattice impurities, except aluminum, via solution–reprecipitation through the liquid

* Corresponding author. Fax: +81-427-21-3624.
E-mail address: hiroshi-yokota@denka.co.jp (H. Yokota).

0955-2219/03/$ - see front matter
PII: S0955-2219(02)00292-3

phase occurs with grain growth,[21,22] so that the use of a high-purity Si_3N_4 raw powder, in particular one with low aluminum and oxygen content, is desirable for producing high thermal conductivity.

Very recently, Kitayama et al.[23] reported that rare-earth oxide additives, although they have no effect on AlN ceramics, significantly change the thermal conductivity of β-Si_3N_4 ceramics. Those researchers demonstrated that mean grain size increases as lattice oxygen content decreases, so that thermal conductivity increases as the ionic radius of the rare-earth element decreases. It has been shown that Yb_2O_3 and Y_2O_3 are suitable additives for improving thermal conductivity of β-Si_3N_4 ceramics.[23,24]

To date, as mentioned earlier, few studies have focused on the technique of microstructural tailoring for high thermal conductivity, other than by merely promoting β-Si_3N_4 grain size. Larger grain sizes lead to lower mechanical strength of the sintered material, because the flaw size becomes larger in relation to the fracture. Thus, a combination of high thermal conductivity and good mechanical properties is not achievable in the presence of abnormally grown grains. Therefore, if high thermal conductivity can be achieved by suppressing abnormal grain growth during sintering, the sintered materials become candidates for highly reliable integrated-circuit substrates.

In a previous work,[25] the sintered materials can be regarded as a two phase composite in which large grains with high thermal conductivity are dispersed within the matrix phase (which contains small β-Si_3N_4 grains and grain-boundary phases) of low thermal conductivity, and the thermal conductivity is controlled by the amount of purified large grains of Si_3N_4. Therefore, sintered materials having the microstructures with certain amount of the large grains should exhibit high thermal conductivity if they are fabricated from high-purity powders sintered with Yb_2O_3 or Y_2O_3 as the sintering additive.

In the present work, equiaxed and relative small grain size of β-Si_3N_4 seeds were introduced into fine and high-purity β-powders (low aluminum and oxygen content) to investigate the relation between microstructure and thermal conductivity in β-Si_3N_4 because too large a difference in particle size between the seed particles and the fine powders would result in abnormal grain growth. Thus, the present study demonstrated the effects on thermal conductivity of suppressing abnormal grain growth, by optimizing sintering additives, and of seeding.

2. Experimental procedure

All of the specimens were prepared from high-purity Si_3N_4 raw powders and sintering aids. The fine β-Si_3N_4 powder (powder F) and coarse β-Si_3N_4 powder (powder C), were specially prepared by the direct nitridation of silicon (Denki Kagaku Kogyo, Tokyo, Japan). Powder F was used for fabricating the fine-matrix grains and powder C as seeds for the microstructural tailoring. These powders consisted of 70 mass% β-Si_3N_4 phase and were similar in purity, as shown in Table 1. The raw Si_3N_4 powder and the seed particles were ball-milled, along with 10 mass% Yb_2O_3 and 2 mass% ZrO_2, using methanol as the solvent, for 3 h. The amounts of added seed particles were 0, 13, 24, 36, 49, 60, 71 and 100 vol.%. After the powder mixtures had been dried, they were prepared for sintering. Powder F was fine, and powder C was coarser than powder F; both powders were equiaxed, with a wide particle-size distribution, as shown in Fig. 1. The seed particles used were approximately twice as large as the particles of the fine powders. This size difference was less than in previous studies,[26,27] because too large a difference in particle size between the seed particles and the fine powders would result in abnormal grain growth.

Approximately 2 g of the dried powder was uniaxially pressed, under 20 MPa, in a die 12.5 mm in diameter. The pellet was then cold-isostatically pressed (CIPed) under a pressure of 200 MPa. The CIPed pellet was placed in a BN crucible. Sintering was performed in a graphite furnace at 1950 °C, for 16 h, under a nitrogen pressure of 0.9 MPa. The densities of the specimens were measured by the Archimedes method. The microstructure of the sintered materials was examined by scanning electron microscopy (SEM, JSM-820, JEOL, Tokyo, Japan) of polished and CF_4 plasma etched surfaces.

To evaluate the thermal conductivity, disks 10 mm in diameter and 3 mm thick were cut from the sintered materials. Thermal conductivity at room temperature was calculated using the equation

$$K = \alpha C_p \rho \quad (1)$$

The thermal diffusivity (α) and the specific heat (C_p) of the specimens were measured at room temperature, by the laser-flash method, using a thermal-constant analyzer (Model TC-3000, ULVAC Japan, Ltd., Tokyo, Japan). The specific heat (C_p) was about the same, independent of the sintering time. Therefore, the average value of 0.67 $J\cdot(g\cdot K)^{-1}$ was used in this work.

Table 1
Properties of raw Si_3N_4 powder

Property	Powder C	Powder F
α-Phase content/mass%	30.5	30.2
Purity		
Oxygen/mass%	0.75	0.79
Aluminum/ppm	120	120
Calcium/ppm	70	50
Iron/ppm	40	40
BET specific surface area/$m^2\ g^{-1}$	6.9	15.9

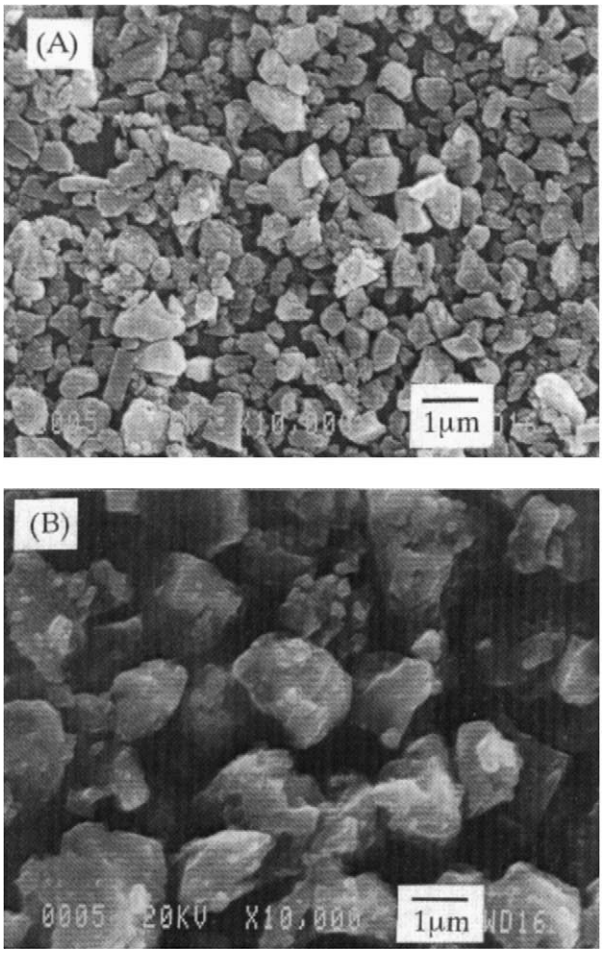

Fig. 1. SEM photograph of (A) fine, raw β-Si_3N_4 powders and (B) large β-Si_3N_4 particles for seeds.

Phase identification of the sintered materials was performed by X-ray diffractometry (XRD).

3. Results and discussion

3.1. Effect of seeding on microstructure

Two different SEM images were employed for one specimen. Fig. 2 shows SEM photographs of the polished and plasma-etched surfaces of the sintered specimens, which were observed at low magnification of 350× to evaluate relatively large grains (⩾2 μm).

Fig. 3 also shows SEM photographs of the sintered specimens, which were observed at high magnification of 2000× to evaluate smaller matrix grains (<2 μm). All specimens had a bimodal microstructure consisting of a lot of fine matrix grains and a number of large elongated grains. For non-seeded specimen, few very large grains (⩾10 μm) selectively grew in the bimodal microstructure. But for seeded specimens, a number of large grains grew in the bimodal microstructure. Digital processing and analysis were performed to quantitatively characterize the microstructure with the wide-ranged grain size distribution. The two SEM images with the different magnification for one specimen were analyzed by image processor to measure length (longest dimension), diameter (shortest dimensions), and area fraction of each grain, and then synthesized into one distribution.[28]

Fig. 4 shows the grain size distribution of the sintered materials. The bimodal microstructure was also confirmed by the grain size distribution. Two peaks with the grain size of <2 μm and ⩾2μm were observed. The lower peak corresponds to the matrix grains and the upper peak corresponds to large elongated grains in the bimodal microstructure. These figures also show that the sizes of the largest grains in the distribution decreased with seeds amount. These results indicate that the coarse additive grains operated by suppressing the growth of very large grains (⩾10 μm).

Table 2 summarizes the seed amounts, densities, aspect ratio (the grain size of <2 μm and ⩾2μm), mean diameter (the grain size of <2 μm and ⩾2μm), area fraction of large grains, and the thermal conductivity of the sintered materials. The aspect ratio between the matrix grains and the large grains were almost the same value. The mean diameter of the matrix grains slightly increased with seed amount, but the mean diameter and the area fraction of the large grains decreased with the seed amount. As shown, the addition of seeds to the raw powder significantly affected the microstructures of the sintered materials.

Fig. 5 shows the relationship between the amount of coarse grains and the mean diameter of the large grains. The diameters of the large grains were largest for the specimen without seeds and then decreased monotonically, and drastically, as the amount of added seeds increased to ~70 vol.%. Figs. 2–5 indicate that the addition of seed particles to the raw powder suppressed abnormal grain growth.

Emoto and Mitomo[27] have revealed that the driving force for abnormal grain growth might depend on the situation of the effective space around a grain. Because few nuclei exist in the fine raw powder (e.g. powder F in the present case), each nucleus has a supersaturated effective space around a grain.[27] This situation leads to abnormal grain growth. Therefore, the significant rnicrostructural change is attributable to the nuclei supplied to the fine, raw powder.

Fig. 6 shows the relationship between the amount of coarse grains and the area fraction of large grains. The area fraction of large grains also decreased as the seed amounts increased. The area of large grains was ~40%, even for 100 vol.% seed addition.

Fig. 7 shows the relationship between the area fraction and the mean diameter of the large grains. The mean diameter of the large grains decreased as their area fraction decreased. The specimen without seeds exhibited both the largest mean grain size and the largest area fraction of large grains. The specimen with 24 vol.%

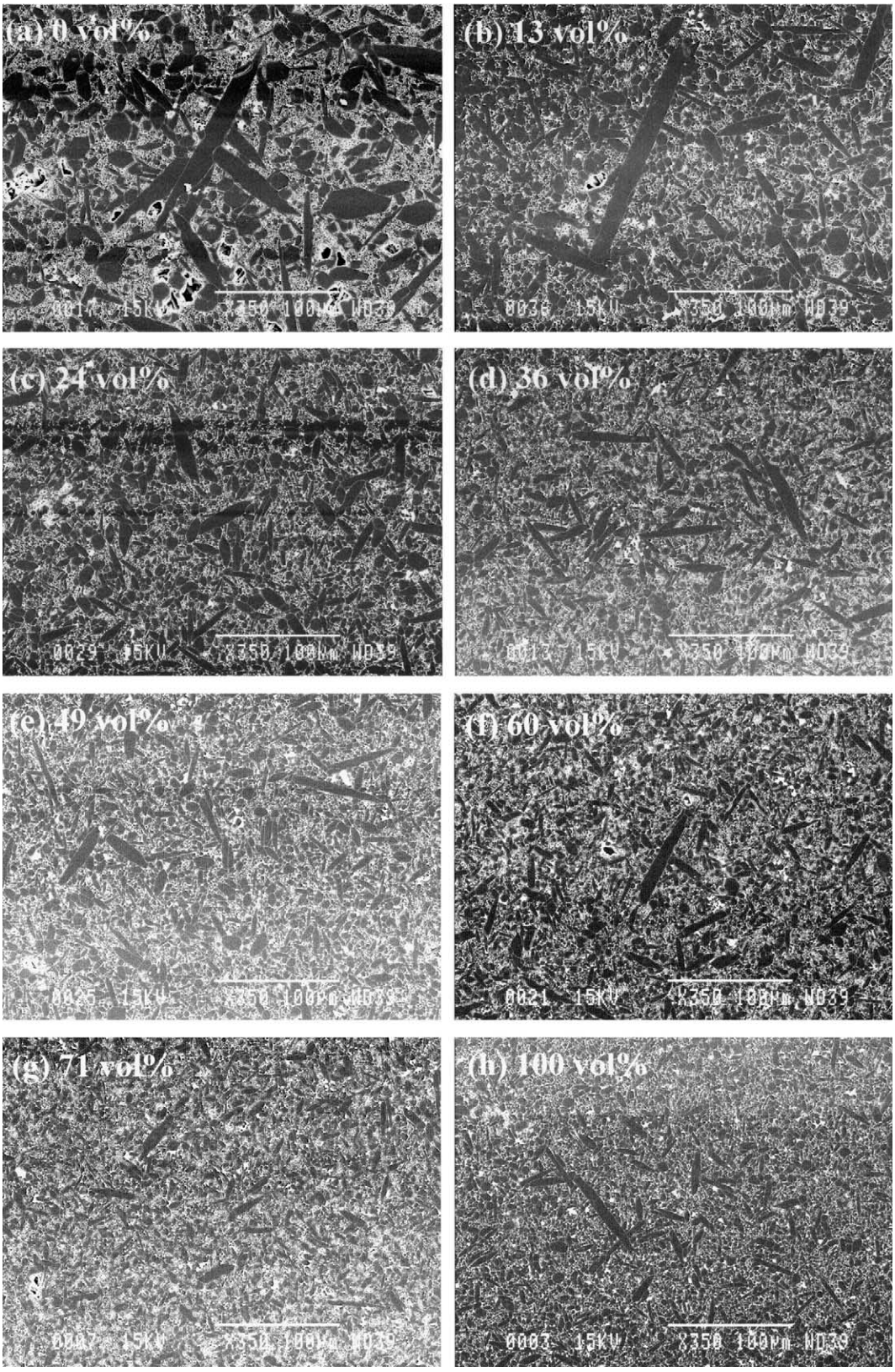

Fig. 2. Low magnification SEM photographs of polished and plasma-etched surface of the specimens sintered at 1950 °C for 16 h of (a) without the seed particles (b) with 13 vol.% added (c) with 24 vol.% added (d) with 36 vol.% added (e) with 49 vol.% added (f) with 60 vol.% added (g) with 71 vol.% added (h) with 100 vol.% added.

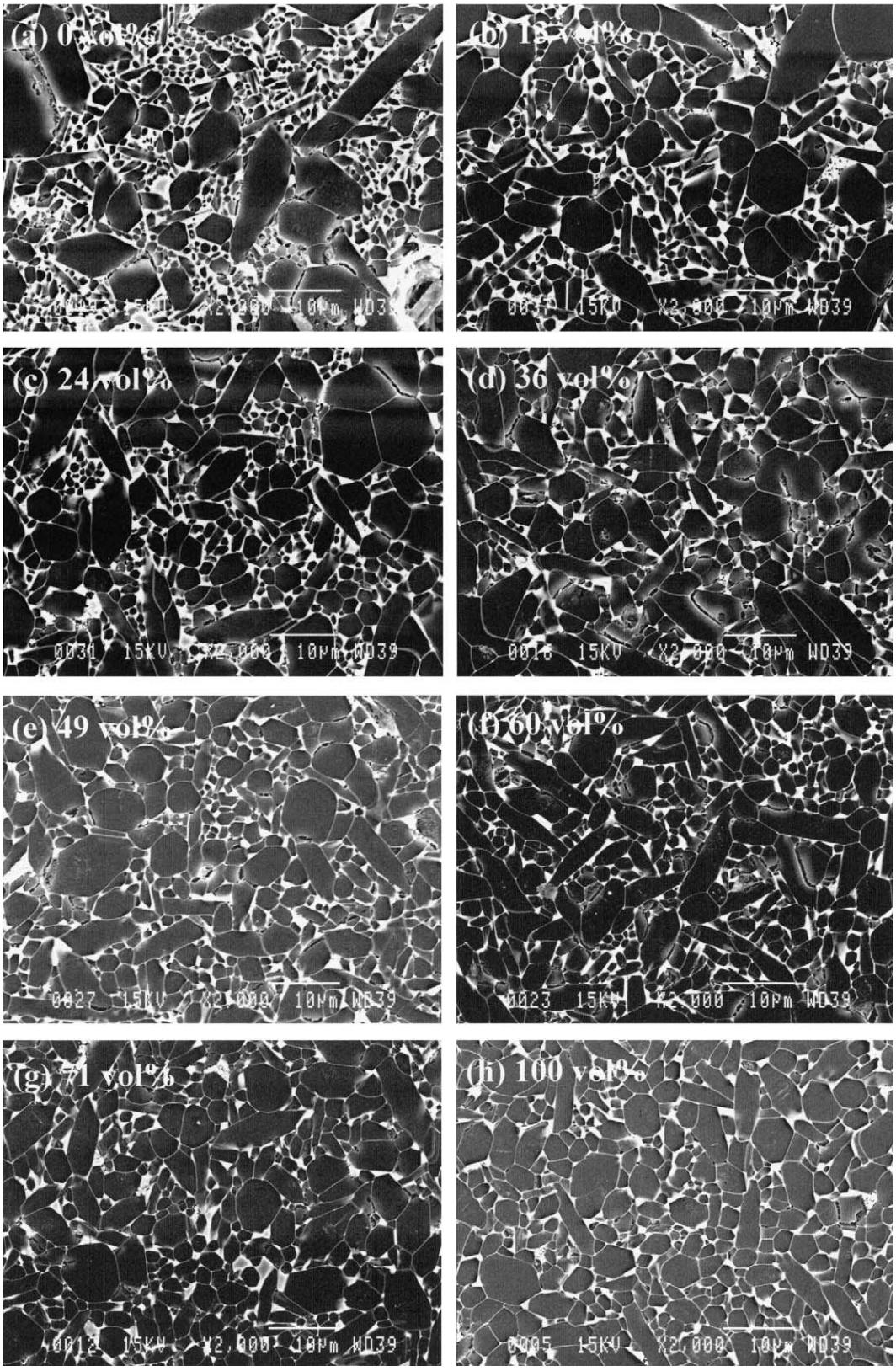

Fig. 3. High magnification SEM photographs of polished and plasma-etched surface of the specimens sintered at 1950 °C for 16 h of (a) without the seed particles (b) with 13 vol.% added (c) with 24 vol.% added (d) with 36 vol.% added (e) with 49 vol.% added (f) with 60 vol.% added(g) with 71 vol.% added (h) with 100 vol.% added.

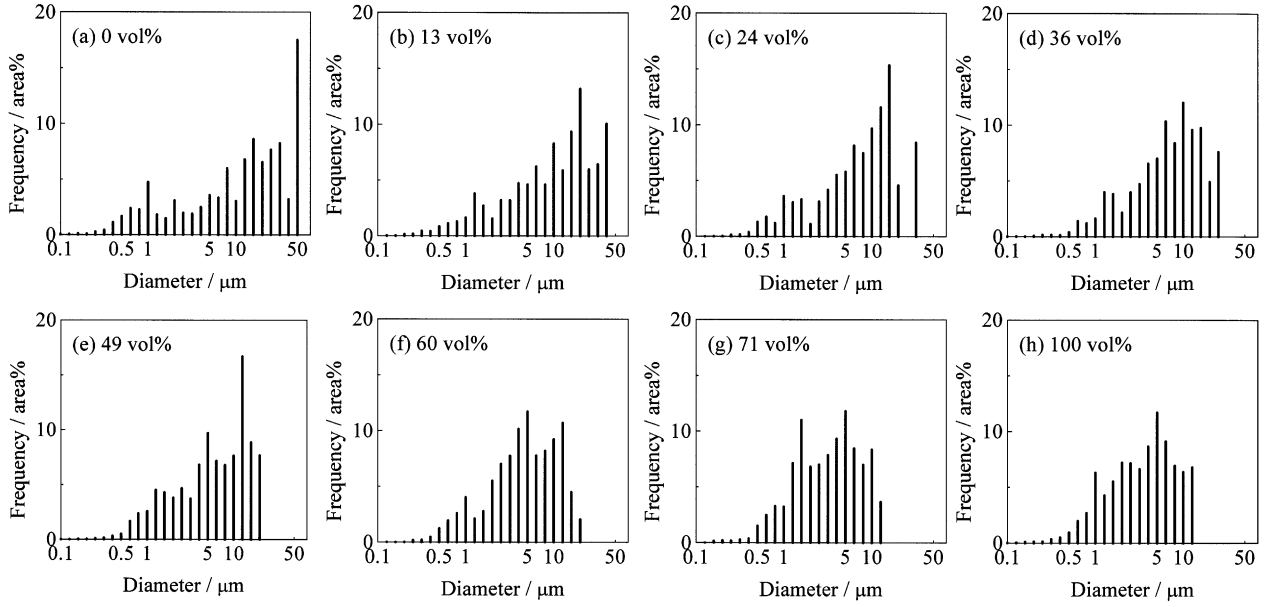

Fig. 4. Grain size distribution of the sintered materials of the specimens sintered at 1950 °C for 16 h of (a) without the seed particles (b) with 13 vol.% added (c) with 24 vol.% added (d) with 36 vol.% added (e) with 49 vol.% added (f) with 60 vol.% added (g) with 71 vol.% added (h) with 100 vol.% added.

Table 2
Seed amount, density, aspect ratio of matrix grains and large grains, mean diameter of matrix grains and large grains, area fraction of large grains, and thermal conductivity of the sintered materials

Seed	Amount (vol.%)	Density (g/cm^3)	Aspect ratio		Mean diameter		Area fraction of large grains (area%)	Thermal conductivity $W\cdot(m\cdot K)^{-1}$
			Matrix (μm)	Large (μm)	Matrix (μm)	Large (μm)		
(a)	0	3.41	3.9	3.9	1.1	17.2	57.1	140
(b)	13	3.39	3.4	3.7	1.1	13.2	56.5	141
(c)	24	3.40	3.6	3.4	1.2	9.5	56.7	142
(d)	36	3.39	3.4	3.5	1.3	8.2	51.5	138
(e)	49	3.40	3.1	3.6	1.4	8.2	43.5	135
(f)	60	3.40	3.2	3.2	1.4	5.5	44.5	135
(g)	71	3.40	3.6	4.2	1.4	4.6	39.7	127
(h)	100	3.40	4.0	3.9	1.4	2.1	38.9	128

seed addition exhibited approximately the same area fraction of large grains as that of the specimen without seeds, but the mean diameter of the large grains was much smaller than in the specimen without seeds (indicated by the arrow in Fig. 7).

Thus, seeding with appropriate amounts of particles allowed the development of microstructures in which certain amounts of large grains could be maintained as the mean diameter of the large grains decreased. Hence, sintered β-Si_3N_4 materials with an extremely wide range in both amount and size of large grains were successfully obtained. Accordingly, the addition of seeds to fine powders suppressed abnormal grain growth while maintaining a certain amount of large grains.

For all of the sintered materials, the $Yb_4Si_2O_7N_2$ (J) phase and the $Zr_4Yb_4O_{12}$ phase were identified. Thus, the grain-boundary phases of the sintered materials were independent of microstructure in the present work.

2.2. Effect of seeding on thermal conductivity

Fig. 8 shows the relationship between the amount of coarse grains and the thermal conductivity of the sintered materials. The thermal conductivities of the sintered materials without the coarse grains and with 13 and 24 vol.% addition of coarse grains were >140 $W\cdot(m\cdot K)^{-1}$ and then gradually decreased as the amount of coarse grains increased.

2.3. Relationship between microstructure and thermal conductivity

Fig. 9 compares the calculated and experimental results for the thermal conductivities of specimens with and without seeds for the sintered materials. The thermal conductivities, K, of the sintered materials are expressed by the following three equations,[25] when we

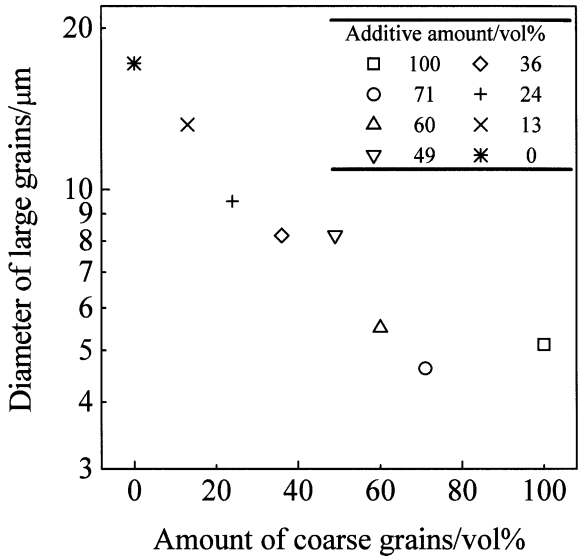

Fig. 5. Relationship between the amount of coarse grains and the mean diameter of the large grains.

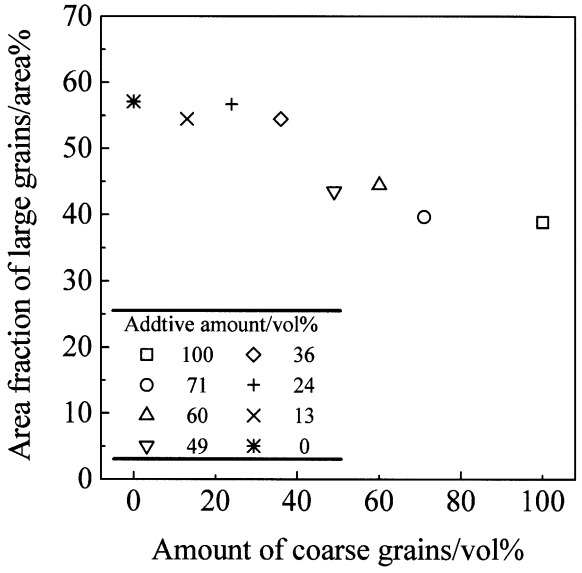

Fig. 6. Relationship between the amount of coarse grains and the area fraction of the large grains.

assume the microstructures of the sintered materials as the two-phase composite material which is composed of the large grains (⩾2 μm) as a dispersed phase and matrix phase (small grains and the grain boundary) as a continuous phase (aspect ratio, $\chi = 3.7$, is chosen as the mean value of the large grains of all specimens in Table 2).

$$K = K_L + \frac{V_L\{A^0\}(K_L - K_M)}{(1 - V_L) + V_L\{A^0\}} \tag{2a}$$

$$3\{A^0\} = \sum_{k=1}^{3} \frac{K_M}{K_M + S^{(K)}(K_L - K_M)} \tag{2b}$$

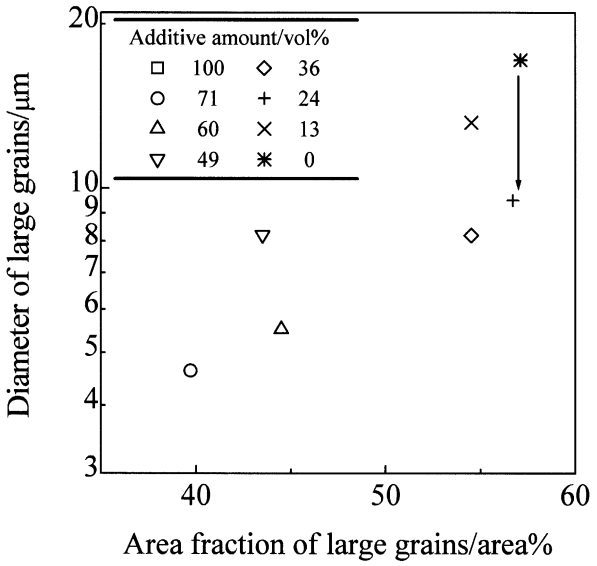

Fig. 7. Relationship between the area fraction of the large grains and the mean diameter of the large grains.

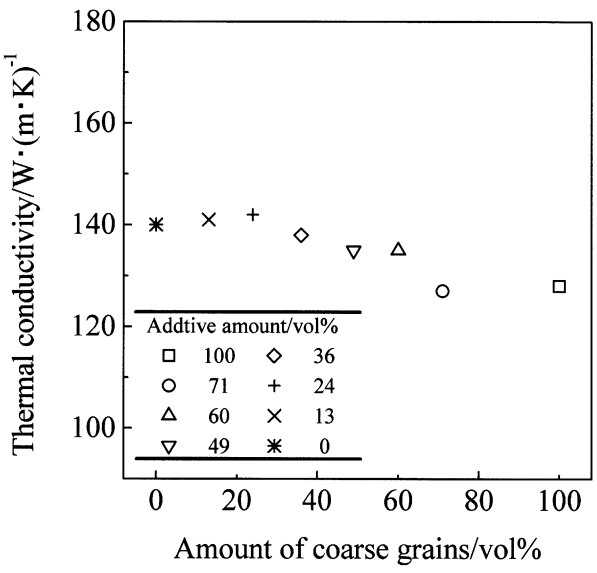

Fig. 8. Relationship between the amount of coarse grains and the thermal conductivity of the sintered materials.

$$S^{(3)} = 1 - 2S^{(1)},\ S^{(1)} = S^{(2)}$$

$$= \frac{(x/2)\left[x\sqrt{x^2-1} - \cosh^{-1}x\right]}{\left(\sqrt{x^2-1}\right)^3} \tag{2c}$$

where K_L, K_M, V_L, $\{A^0\}$, S^K, and χ are the thermal conductivity of the large grains (⩾2 μm), the thermal conductivity of the matrix phase, the volume fraction of the large grains, average value of the concentration factor, shape factor of the large grains, and the aspect ratio of the large grains, respectively.

Fig. 9 shows that the thermal conductivities of the β-Si_3N_4 increased as the amount of large grains

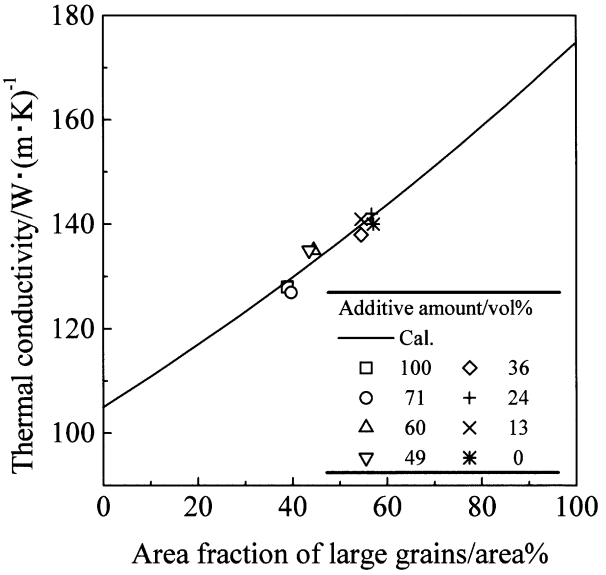

Fig. 9. Comparison of the calculated and experimental results of the thermal conductivities for without seed specimens and with the addition of seeds for sintered materials.

increased. All of the data points scattered along the lines (indicated by the line designated "cal" in Fig. 9) are derived from Eqs. (2a–c), which were independent of the seed amounts. The K_M values (which should represent the thermal conductivity with 0 area% of large grains) possessed a high thermal conductivity, 105 W·(m·K)$^{-1}$, given the K_L value (which should represent the thermal conductivity with 100 area% of large grains) of 175 W·(m·K)$^{-1}$. This result suggests that the reprecipitated large grains ($\geqslant$2 μm) have a higher thermal conductivity because of its purity.

Fig. 10 shows the relationship between the mean diameter of the large grains and the thermal conductivity

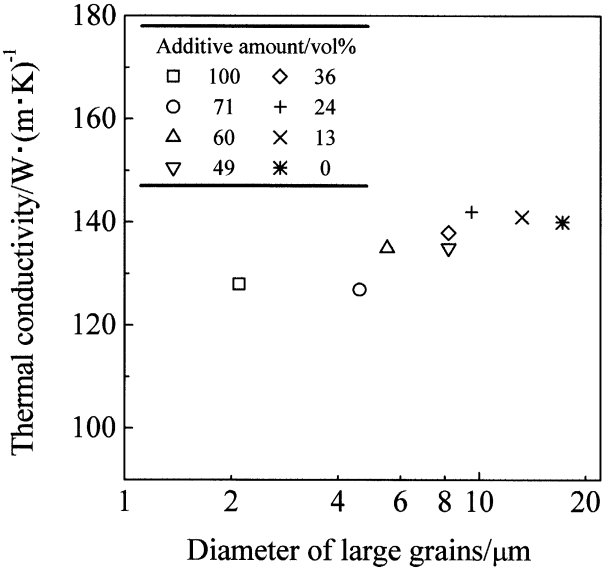

Fig. 10. Relationship between the mean diameter of the large grains and thermal conductivities of the sintered materials.

of the sintered materials. The thermal conductivities of the specimens obtained in this work were independent of the mean diameter of the large grains, except in the specimens with 4–5 μm in mean diameter.

Figs. 9 and 10 indicate that the high thermal conductivity of β-Si_3N_4 with Yb_2O_3 is attributable to the amount of precipitated large grains, rather than to the grain size. In other words, materials sintered with Yb_2O_3 do not need a significantly large grain size to exhibit high thermal conductivity. This finding indicates that thermal conduction of Si_3N_4 ceramics sintered with Yb_2O_3 additive was influenced far less by the grain-boundary.

The present results indicate that using Yb_2O_3 additives for β-Si_3N_4 makes it possible to have high thermal conductivity with appropriate mechanical properties. However, this does not negate the importance of purification-promoted grain growth merely by solution and reprecipitation with the Yb_2O_3 additives, because precipitation of the purified large grains enhances the thermal conductivity of the sintered materials. Indeed, the thermal conductivities of the specimens with grains 4–5 μm in mean diameter were somewhat lower than those of specimens with a larger grain size. This difference resulted from insufficient purification of β-Si_3N_4 grains in the smaller-grained specimens.

4. Conclusions

High-purity β-Si_3N_4 powders with or without added β-Si_3N_4 particles (seeds) were gas-pressure sintered at 1950 °C for 16 h, using Yb_2O_3 and ZrO_2 as sintering aids, and the microstructures, thermal conductivities, and grain-boundary phases of the sintered powders were investigated. The following conclusions were drawn from the present work.

1. All specimens had a bimodal microstructure consisting of a lot of fine matrix grains (<2 μm in diameter) and a number of large elongated grains ($\geqslant$2 μm diameter).
2. Adding β-Si_3N_4 seeds caused a significant change in the microstructure of a gas-pressure-sintered specimen. The mean size of the large grains of β-Si_3N_4 decreased with the seeds amount.
3. Seeding with appropriate amounts of particles allowed the development of microstructures in which certain amounts of large grains were maintained as the mean diameter of the large grains decreased. The grain-boundary phases of the sintered materials were independent of their microstructures.
4. The thermal conductivity of the specimen without seeds was 140 W·(m·K)$^{-1}$, and the specimen exhibited abnormally grown grains. On the other

hand, it was possible to refine the microstructures, having finer grain size than that without the seeded material, maintaining the high thermal conductivities of over 140 $W\cdot(m\cdot K)^{-1}$ by the appropriate amount of seed addition.

5. The relationship between the microstructure and the thermal conductivity of the sintered β-Si_3N_4 revealed that the thermal conductivity of β-Si_3N_4 is independent of grain size but controlled by the amount of reprecipitated large grains.

References

1. Huebner, G. and Knoch, H., Mechanical properties of hot-pressed silicon nitride with different grain structures. *J. Am. Ceram. Soc.*, 1979, **62**(11), 29–32.
2. Becher, P. F., Microstructural design of toughened ceramics. *J. Am. Ceram. Soc.*, 1991, **74**(8), 255–269.
3. Wottig, G., Kanka, B. and Ziegler, G., Microstructural development, microstructural characterization and relation to mechanical properties of dense silicon nitride. In *Non-Oxide Technical and Engineering Ceramics*, ed. S. Hampshire. Elsevier Applied Science, London, 1986, pp. 83–96.
4. Sajglik, P., Dusza, P. and Hoffmann, J., Relationship between microstructure, toughening mechanisms. *J. Am. Ceram. Soc.*, 1995, **78**(7), 2619–2624.
5. Hirosaki, N., Okamoto, Y., Ando, M., Munakata, F. and Akiume, Y., Thermal conductivity of gas-pressure-sintered silicon nitride. *J. Am. Ceram. Soc.*, 1996, **79**(11), 2878–2882.
6. Hirao, K., Watari, K., Brito, M. E., Toriyama, M. and Kanzaki, S., High thermal conductivity in silicon nitride with anisotropic microstructure. *J. Am. Ceram. Soc.*, 1996, **79**(9), 2485–2488.
7. Hirosaki, N., Okamoto, Y., Ando, M., Munakata, F. and Akiume, Y., Effect of grain growth on the thermal conductivity of silicon nitride. *J. Ceram. Soc. Jpn.*, 1996, **104**(1), 49–53.
8. Watari, K., Hirao, K., Brito, M. E., Toriyama, M. and Kanzaki, S., Hot isostatic pressing to increase thermal conductivity of silicon nitride ceramics. *J. Mater. Res.*, 1999, **14**(4), 1538–1541.
9. Akiume, Y., Munakata, F., Matsuo, K., Okamoto, Y., Hirosaki, N. and Satoh, C., Effect of grain size and grains structure on the thermal conductivity of β-Si_3N_4. *J. Ceram. Soc. Jpn.*, 2000, **83**(8), 1985–1992.
10. Lange F. L., Relation between strength, fracture energy, and microstructure of hot-pressed Si_3N_4. 1973, 56(10), 518–22.
11. Lange, F. L., Fracture toughness of as a function of the initial α-phase content. *J. Am. Ceram. Soc.*, 1979, **62**(7–8), 428–433.
12. Mitomo, M., Tsutsumi, T., Tanaka, H., Uesono, S. and Saito, F., Grain growth during gas-pressure sintering of β-silicon nitride. *J. Am. Ceram. Soc.*, 1990, **73**(8), 2441–2445.
13. Mitomo, M. and Uesono, S., Gas-pressure sintering of β-silicon nitride. *J. Mater. Sci.*, 1991, **26**, 3940–3944.
14. Dressler, W., Kleebe, H.-J., Hofmann, M. J., Ruhle, M. and Petzow, G., Model experiments concerning abnormal grain growth in silicon nitride. *J. Eur. Ceram. Soc.*, 1996, **16**, 3–14.
15. Rhee, S.-H., Lee, J. D. and Kim, D.-Y., Effect of heating rate on the exaggerated grain growth behavior of β-Si_3N_4. *Mater. Lett.*, 1997, **32**, 115–120.
16. Lee, S.-J., Kang, L., Rhee, Lee, J. D., Kim, D.-Y., Petzow, G. and Yoon, D. N., Effect of α to β(β′) phase transition on the sintering of silicon nitride ceramics. *J. Am. Ceram. Soc.*, 1990, **73**(3), 767–769.
17. Mitomo, M., Toughening of silicon nitride ceramics by microstructure control. In *Proceedings of the 1st International Symposium on the Science of Engineering Ceramics*, ed. S. Kimuraand and K. Niihara. Ceramic Society of Japan, Tokyo, Japan, 1991, pp. 101–107.
18. Watari, K., Hirao, K., Brito, M. E., Toriyama, M. and Ishizaki, K., Effect of grain size on the thermal conductivity of silicon nitride. *J. Am. Ceram. Soc.*, 1999, **82**(3), 777–779.
19. Kitayama, M., Hirao, K., Toriyama, M. and Kanzaki, S., Thermal conductivity of β-Si_3N_4. Part I, effects of various microstructural factors. *J. Am. Ceram. Soc.*, 1999, **82**(11), 3105–3112.
20. Kitayama, M., Hirao, K., Tsuge, A., Watari, K., Toriyama, M. and Kanzaki, S., Thermal conductivity of β-Si_3N_4. Part II, effect of lattice oxygen. *J. Am. Ceram. Soc.*, 2000, **83**(8), 1985–1992.
21. Yokota, H. and Ibukiyama, M., High-thermal conductivity of β-Si_3N_4 prepared by gas pressure sintering. In *Ceramic Transactions, Vol 112, Ceramic Processing Science IV, 7th International ceramic processing science meeting 2000*, ed. S. Hirano, G. L. Messing and N. Claussen. American Ceramic Society, Westerville, OH, 2001, pp. 611–616.
22. Yokota, H. and Ibukiyama, M., Effect of lattice impurities on the thermal conductivity of β-Si_3N_4. *J. Eur. Ceram. Soc.*, 2002, **23**(1), 55–60.
23. Kitayama, M., Hirao, K., Watari, K., Toriyama, M. and Kanzaki, S., Thermal conductivity of β-Si_3N_4: III, effect of rare-earth (RE = La, Nd, Gd, Y, Yb, and Sc) oxide additives. *J. Am. Ceram. Soc.*, 2001, **84**(2), 353–358.
24. Hayashi, H., Hirao, K., Toriyama, M., Kanzaki, S. and Itatani, K., $MgSiN_2$ addition as a means of increasing the thermal conductivity of β-silicon nitride. *J. Am. Ceram. Soc.*, 2001, **84**(12), 3060–3062.
25. Yokota, H., Yamada, S. and Ibukiyama, M., Effect of amount of β-Si_3N_4 particles on thermal conductivity. *J. Eur. Ceram. Soc.* (submitted for publication).
26. Hirosaki, N. and Mitomo, M., Microstructure characterization of gas-pressure sintered β-silicon nitride containing large β-silicon nitride. *J. Am. Ceram. Soc.*, 1994, **77**(4), 1093–1097.
27. Emoto, H. and Mitomo, M., Control and characterization of abnormally grown grains in silicon nitride ceramics. *J. Eur. Ceram. Soc.*, 1997, **17**, 797–804.
28. Hirosaki, N., Akiume, Y. and Mitomo, M., Quantitative analysis of microstructure of self-reinforced silicon nitride ceramics. *J. Ceram. Soc. Jpn.*, 1993, **101**(11), 1239–1243.